ACADEMIA ROMÂNĂ
Revue Roumaine de Chimie
http://web.icf.ro/rrch/

Rev. Roum. Chim.,
2018, *63*(5-6), 467-474

Dedicated to Dr. Maria Zaharescu
on the occasion of her 80th anniversary

CERIUM MODIFIED MESOPOROUS TiO_2 PHOTOCATALYST OBTAINED BY SOL-GEL METHOD

Teodor DIACONU,[a] Madalina CIOBANU,[a]* Gabriela PETCU,[a] Daniela CULITA,[a] Silviu PREDA,[a] Jeanina PANDELE-CUSU,[a] Mihaela MURESEANU[b] and Viorica PARVULESCU[a]

[a] "Ilie Murgulescu" Institute of Physical Chemistry, Roumanian Academy, Splaiul Independenței 202, 060021, Bucharest, Roumania
[b] Department of Chemistry, Faculty of Sciences, University of Craiova, 107 I Calea Bucureşti, 200478, Craiova, Roumania

Received July 31, 2017

The mesoporous photocatalysts based on ceria supported on TiO_2 were obtained through triblock copolymer (P123)-templated sol-gel method via an evaporation-induced self-assembly process. The obtained nano-sized oxide was impregnated with different percentages of CeO_2. The obtained photocatalysts with 5, 7.5 and 10 % CeO_2 were characterized by X-ray diffraction, thermal analysis, SEM microscopy, N_2 adsorption-desorption, UV-Vis spectroscopy and tested in photocatalytic degradation of methyl orange from aqueous solution. The obtained results have confirmed the synthesis of mesoporous titania oxide with anatase crystalline structure, narrow pore size distribution and high surface area. A spherical morphology and an arrangement of nanoparticles, typically for mesoporous material, were evidenced by SEM microscopy. Degradation of methyl orange was correlated with composition, band gap energy, wavelenght of the light irradiation and time of reaction. The modification of TiO_2 sample surface by cerium oxide decreased its photocatalytic performance in degradation of MO dye under UV light and increased the photocatalytic efficiency in visible light. The best results in photodegradation of MO were obtained for 5% CeO_2 concentration in modified samples.

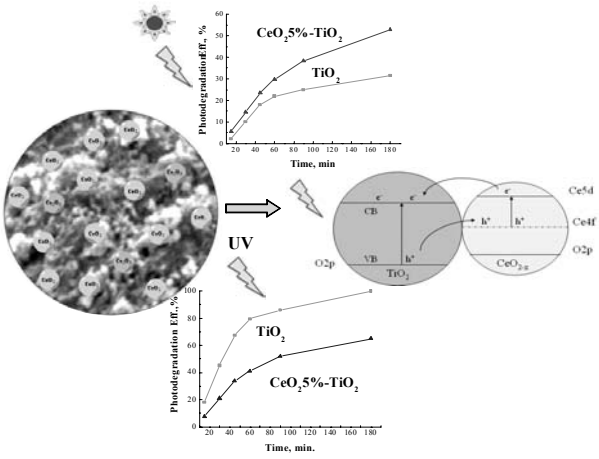

INTRODUCTION

Photocatalysis attracts great attention because it has promising applications in degradation of various pollutants and conversion of the light energy into chemical energy, domains of great interest. For photocatalytic applications, crystalline titania is an interesting semiconductor much preferred. TiO_2 exists in different polymorphs, the most common forms are the anatase- and rutile-crystal structures.[1] Generally, anatase (A) is more active than rutile (R) in condition of its higher band gap value (A- 3.2 eV; R- 3.0 eV). This difference was explained by bulk transport of excitons to the surface.[2] Furthermore, rutile is the most thermodynamically stable of the three polymorphic phases. Many studies showed that between the isolated phases, their mixtures and

* Corresponding author: mciobanu@icf.ro

heterojunction were revealed differences in photocatalytic activity. Thus, mixed anatase/rutile TiO_2 was proved to be more active than pure anatase and rutile[3], mixed phase brookite/rutile exhibited a superior photoactivity compared to Degussa P25 and anatase phase.[4] Other studies shown that anatase/brookite is more active than anatase, brookite and anatase/rutile in the photocatalytic oxidation of organic compounds.[5,6]

Titania-based photocatalysts were synthesized by various methods, but sol-gel process was the most used due its some advantages, such as homogenity at molecular level, a wide range of a precursor selection, control over microstructure, possibility of a fine adjustment of the end product properties, simplicity of process, low temperature and cost.[7-12] Mesoporous crystalline materials based on titanium dioxide have been successfully synthesized via a simple and cheap surfactant assisted sol-gel method using titania hydrosols and different organic templates as starting materials.[13-16] The mesoporous structure of TiO_2 is of particular interest because the mesoporous channels offer a large surface area, and the pore wall framework is nanocrystalline. In addition, the thermal stability of mesoporous TiO_2 is better than that of traditional TiO_2 nanoparticles. Antonelli et al. were the first who synthesize mesoporous titania using a surfactant-templated process.[17] However, the effects of P123 templating agent and cosurfactant (1-butanol) in the synthesis of mesoporous nanocrystalline anatase TiO_2 on gelation process that must be avoided before the formation of the ordered mesoporous structure were explained later.[18]

The band gap of TiO_2, which is 3.2 eV for anatase and 3 eV for rutile, is capable to sustain chemical reactions as degradation of organic compounds from water and air or even water spliting but it is at high border of visible domain, so disposing a limitative quantity of sunlight in case of large scale depoluation. Between the strategies to modify TiO_2 for the utilisation of the visible spectrum, besides dye sensitizers, are doping with metallic and nonmetallic elements, and also coupling to another semiconductor.[19-21]The doping metal ions can also increase the catalytic activity by formation of a better active center. Among the large number of studies related to TiO_2 doping with other metal oxides the coupling of titania oxide with ceria are attracting much attention.[22-24] Making a confirmed increasing of catalytic activity[25]cerium is an interesting candidate to TiO_2 array doping due same valence in the stable oxide and and having four valence electrons both, but different in the ion radius (115 pm for Ce^{3+} and 101 pm for Ce^{4+} opposite to 81 pm fot Ti^{3+} and 74.5 pm for Ti^{4+}).[24,26] Whereas stable state of cerium oxide is CeO_2, which have a distinct crystalisation geometry, for TiO_2-CeO_2 mixed oxide, which shows an absorbtion in the visible, was reported a decrease in oxidation state.[27-31] Also, an adition of CeO_2 in structure less than 10% will increase the porosity and stability at calcination.[20] The cerium oxide is attractive in view of its optical and catalytic properties, connected with the presence of the ion couple Ce^{3+}/Ce^{4+} and with the ability to store non-stoichiometric oxygen and release it in oxidation reactions.[32] Owning the 5d level, CeO_2 is a transparent semiconductor oxide with E_g = 3.19 eV for the nanocristalline form, which is reported to be decreased to 2.75 eV.[26, 33]

In this study the mesoporous photocatalysts based on TiO_2 modified with CeO_2 were obtained through triblock copolymer-templated sol-gel method via an evaporation-induced self-assembly (EISA) process. The percent of CeO_2 will be no more than 10% in order to obtain a group of materials with band gap drop to visible domain, a stable porous structure to calcination, formation of stable anatase structure and a high specific surface and narrow pore size, properties with high influence in the degradation of pollutants like dyes from water.

RESULTS AND DISCUSSIONS

Mesoporous TiO_2 has been synthesized through triblock copolymer templated sol-gel method via an evaporation-induced self-assembly (EISA) process. The sol-gel was carried out in the presence of Pluronic P123 as the structure directing agent and propanol as solvent and co-surfactant. The obtained oxide was impregnated with different percentages of CeO_2 (5,7.5 and 10 wt %, respectively).

The thermogravimetric results (Fig. 1) indicate, for TGP sample, three intervals of temperature in which mass variation takes place. Thus, up to 200^0C there is a weight loss of only 10% as result of solvents evaporation, between 200^0C and 300^0C can be observed a significant mass decreasing (around 50%) as result of thermal decomposition of the surfactant. After this, the weight loss is very low (10%) due to the formation of TiO_2 crystalline structure. After impregnation, thermal analysis indicates a continuous drop in mass up to 400^0C with a ramp tendency between 200^0C and 300^0C. The weight loss varied with cerium precursor content. As a result of these observations we have established the program for the thermal treatment of the synthesized samples.

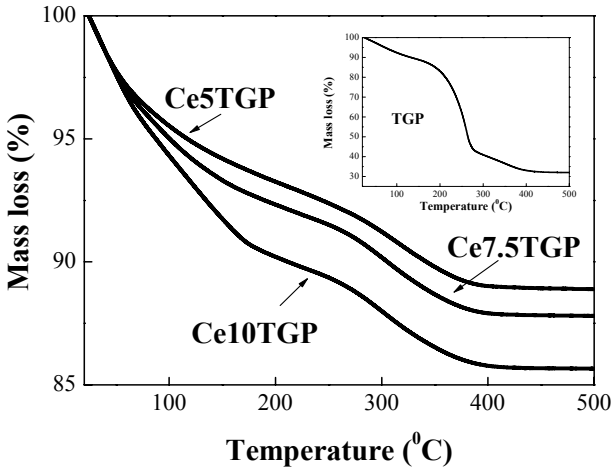

Fig. 1 – Thermal analysis for TGP, Ce5TGP, Ce7.5TGP, Ce10TGP samples.

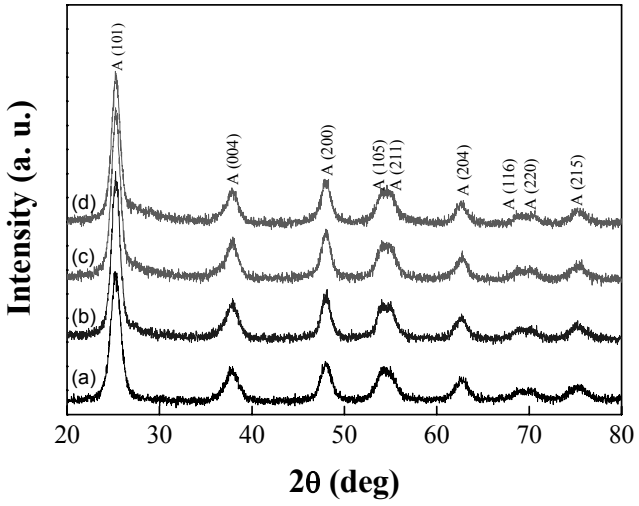

Fig. 2 – XRD patterns of mesoporous TiO_2 (a) TGP; (b) Ce5TGP; (c) Ce7.5TGP; (d) Ce10TGP samples.

After thermal treatment in air at 400 ^{o}C the diffraction patterns were indexed to the anatase phase for all the samples (Fig. 2). The XRD peaks of ceria in the synthesized CeTGP samples are not defined. The reasons for this fact are both the low content of CeO_2 in the composite (5 wt.%), as well as the possibility that the Ce species are highly dispersed and are not incorporated into the TiO_2 lattice.

N_2 adsorption-desorption isotherms and pore size distributions of the prepared samples (Fig. 3) show a type IV isotherm with a H2 hysteresis loop in which the desorption branch is less steep and adsorption branch is more sloping. This type of isotherms correspond to materials more disordered where the distribution of pores (Fig. 3) is not very narrow, the shape is not well defined and also are posible bottleneck constrictions. The mesoporous TiO_2 has a surface area of 141 m^2g^{-1} and pore volume of 0.24 cm^3g^{-1}. The previous results[34] showed that the catalyst specific surface area, degree of crystallinity and metal nanoparticle size on the oxide surface are the factors that can affect significantly the efficiency of photodegradation of organic contaminants from water. The obtained results evidenced the synthesis of mesoporous TiO_2 with surface area considerably higher than that of many others TiO_2 oxides.[26]

After the impregnation with CeO_2 the surface area and the pore volume decreases along with the increase of CeO_2 quantity (Table 1, Fig. 3). A slightly wider pore size distribution was obtained for all the samples and a low shift of pore size to lower values with increasing of CeO_2 concentration was observed for all the samples. This is result of cerium penetration into the pores.

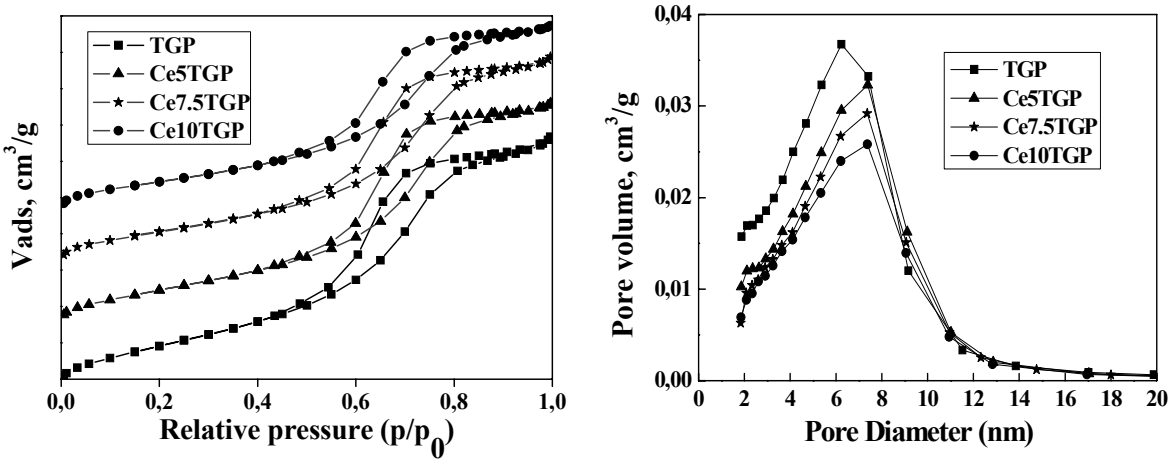

Fig. 3 – Nitrogen adsorption-desorption isotherms (left) and pore size distribution (right) of the synthesized mesoporous materials.

Table 1

Textural and optical properties of mesoporous TiO_2 impregnated with different CeO_2 concentrations

Samples	S_{BET}, m^2/g	Vp, cm^3/g	Dp, nm	Band gap, eV
TGP	141	0.24	5.66	3.01
Ce5TGP	116	0.21	5.27	2.32
Ce7.5TGP	102	0.19	5.38	2.30
Ce10TGP	94	0.17	5.23	2.29

S_{BET} – surface area; Vp – pore volume; Dp – pore diameter

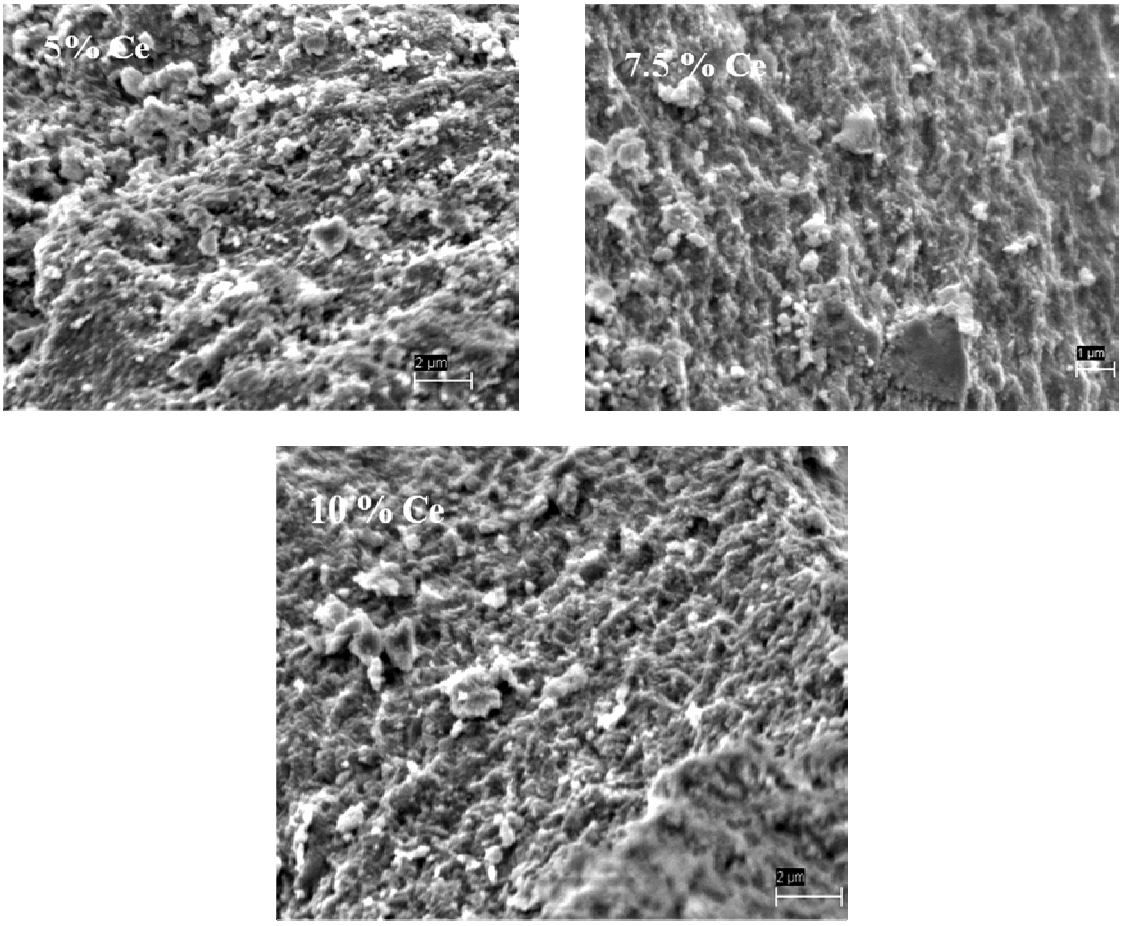

Fig. 4 – SEM images of TGP samples with 5, 7.5 and 10 % ceria.

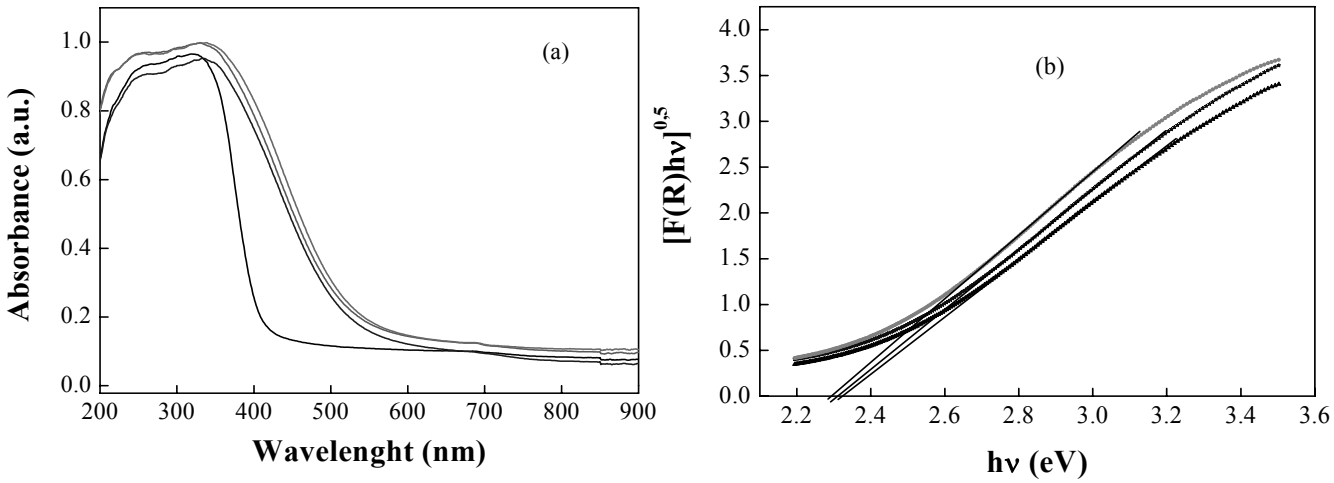

Fig. 5 – UV-Vis absorption spectra (a) and (b) plot of transferred Kubelka-Munk vs. Energy of the light absorbed.

The band gap value was determined from the intersection of tangent through the point of inflexion in the absorption band and the photon energy axis (Fig. 5(b)). Cerium ions narrow the band gap of TiO_2 and improve the absorption. Comparing the band gap energy of CeTGP samples with the respective energy of pure titania (TGP sample) can be observed the shift toward visible light region. This is in accordance with results reported by other authors.[26] The low effect of CeO_2 loading on band gap was considered result of cerium agglomeration in condition of an insignificant increasing of TiO_2/CeO_2 interface.

Nevertheless, the results of the photocatalytic tests indicate a significant variation of MO photodegradation efficiency for samples with a CeO_2 concentration greater than 5% (Fig. 6). After 7.5% CeO_2 loading an insignificant decreasing of photodegradation efficiency was observed. We believe that under these conditions the dispersion of CeO_2 decreases significantly.

The sample with a higher photocatalytic activity (Ce5TGP) and TGP support were tested in the degradation of methyl orange in aqueous solution ($1x10^{-5}$ M) by irradiation with UV and visible light at room temperature. The obtained results are presented in Figure 7.

Fig. 7a shows a very high photodegradation efficiency of MO in UV light for TGP sample with pure TiO_2 and a lower for Ce5TGP sample.

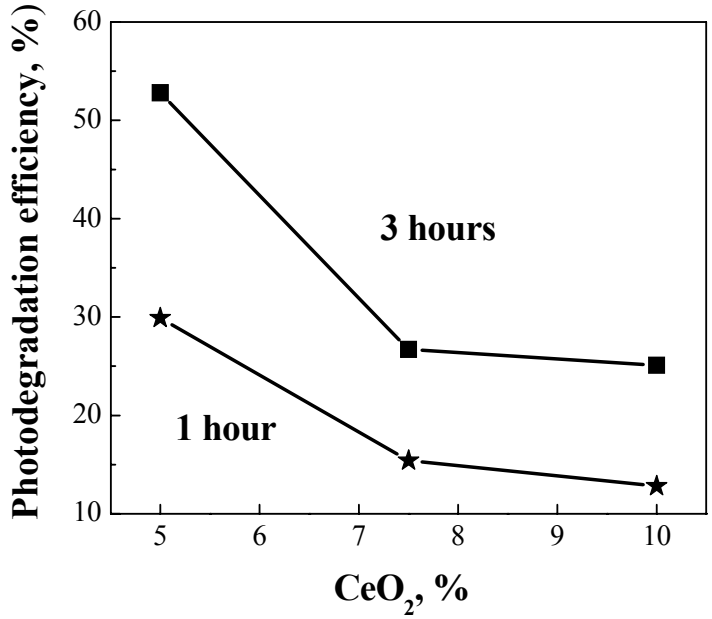

Fig. 6 – The variation of MO photodegradation efficiency with ceria content under visible light.

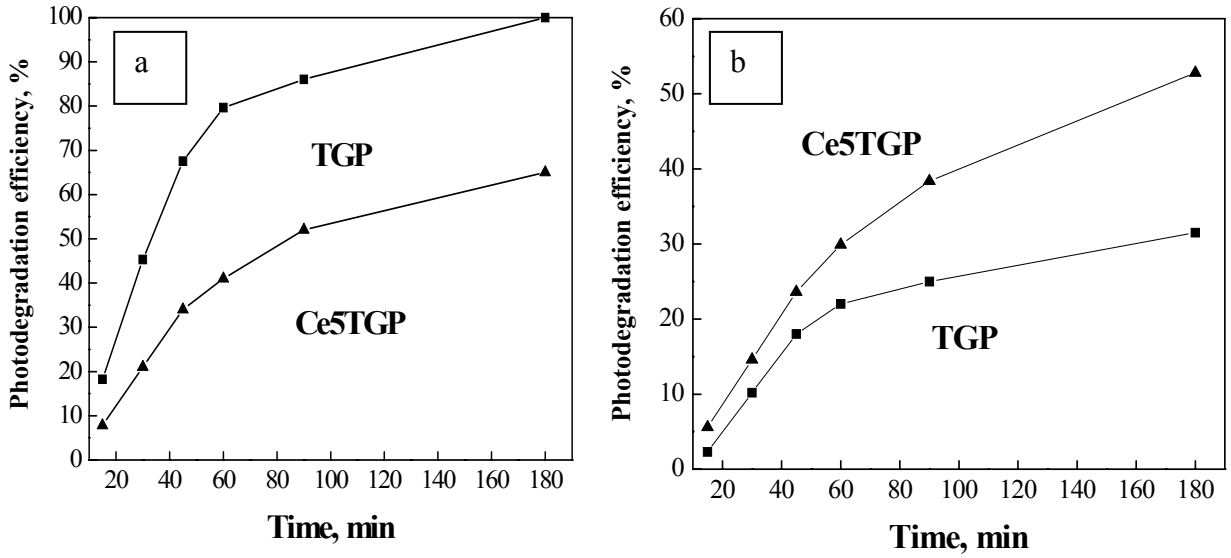

Fig. 7 – Photocatalytic performances of TGP and Ce5TGP samples under UV (a) and visible light (b).

The photocatalytic performance of CeTGP sample in MO degradation under UV or visible irradiation is related to the effectiveness of charge carrier separation in the photoexcited semiconductor material, larger specific surface area and greater number of surface hydroxyl groups of the samples.[26,36] Compared to the results obtained in UV, in condition of the visible light irradiation, at room temperature, it was found that the MO photodegradation efficiency is lower for TGP sample and slightly higher for Ce5TGP sample (Fig. 7b). In the presence of visible light CeO_2 phase is excited, the TiO_2 phase remaining unactivated.[26] Nevertheless, in the presence of cerium MO photodegradation efficiency on TGP sample under visible light irradiation was much lower than those measured in the case of UV light (Fig.7).

From the UV absorption spectra we evidenced two characteristic absorption peaks located at 464 nm and 271 nm, arising from the "–N = N–" azo bonding and benzene ring of MO, respectively. The literature shows that the –N = N– bonding is completely decomposed, corresponding to the disappearance of orange color in the solution. MO photodegradation to inorganic compounds (H_2O and CO_2) was observed after a longer time of irradiation (over 24 hr).[37]

EXPERIMENTAL

1. Materials

Titanium butoxide (TBOT), hydrochloric acid solution (38%), n-propyl alcohol, the block copolymer surfactant $EO_{20}PO_{70}EO_{20}$ (Pluronic P123, M_n ~5,800), $Ce(NO_3)_3{\cdot}6H_2O$, methyl orange (MO) were purchased from Sigma Aldrich. All chemicals used in this work were of analytical grade and were used without further purification.

2. Preparation of mesoporous Ce-TiO_2

The synthesis of mesoporous TiO_2 was carried out by sol-gel method in presence Pluronic block copolymer surfactant. In a mixture of P123 and n-propyl alcohol was added 5.35 ml HCl solution (5,4 M) and sttirred for three hours, then TBOT (8 mL) was added dropwise. After two hours the mixture was poured in Petri glasses and let it overnight for gelling at 35-40^oC. When the gel had the proper consistency, it was detached and dried at 80^oC overnight. After that, the gel was crushed, calcined and finally milled. The inorganic material was calcined in air at 400°C for 8h at a heating rate of 2^oC min^{-1}. After calcination the material was impregnated with cerium nitrate solution, dried and calcined in similar conditions to obtain samples with 5, 7.5 and 10 wt. % CeO_2 concentration named Ce5TGP, Ce7.5TGP and Ce10TGP.

3. Measurements of Photocatalytic Activities

The photocatalytic degradation of methyl orange (MO) dye in aqueous solution was performed in a quartz microreactor using TGP and Ce5TGP photocatalysts under visible (380-750 nm) or UV radiation (filter for λ=254 nm) for 1, 3 and 5 h, respectively. 8 mL MO dye solution ($1x10^{-5}$M) and 1.5 mg photocatalyst were aded in a quartz reactor. Before irradiation, the suspensions were magnetically stirred in dark for 30 min to stabilize the adsorption of MO dye over the photocatalyst surface. Then, the reactor was exposed to irradiation under ambient conditions and under stirring. At specific time intervals, the suspension (3ml) was taken out and filtrate in order to separate the catalyst. The degradation process was evaluated by the strength of the maximum absorbance of MO at 464 nm absorption peak (JASCO V-570 UV-VIS spectrometer). The degradation rate was calculate using the relation $(A_0\text{-}A)/A_0*100$, where A_0 is the initial absorbance and A the absorbance value after the photodegradation.[37]

4. Characterization

Powder X-ray diffraction (XRD) measurements were performed on a Bruker AXS D8 diffractometer by using Cu Kα radiation (λ= 0.154 nm) over a 2θ range from 20° to 80°

and N_2 adsorption–desorption isotherms were measured at -196°C with a Micromeritics ASAP 2010 instrument. The samples were previously degassed under vacuum at 50°C for 12 h. Specific surface area was calculated by the BET method and the mesopore volume was determined from the isotherm at the end of capillary condensation. The pores size distribution was obtained from the desorption branch using the BJH method and the Harkins-Jura standard isotherm. The thermal analysis was investigated by using Mettler Toledo TGA/DTA 851e apparatus, from room temperature up to 500°C and the heating rate was of 2°C/min. The measurement was performed in air atmosphere (gas flow 80ml/min). The morphology of the sample was investigated by scanning electron microscopy (SEM) using a high-resolution microscope, FEI Quanta 3D FEG model and UV–vis spectra were recorded on JASCO V-570 UV-VIS Spectrophotometer.

CONCLUSIONS

The mesoporous TiO_2 was obtained by sol-gel method in the presence of nonionic structure directing agent (P123) and propanol as solvent. The obtained oxide was modified with cerium leading to materials with 5, 7.5 and 10 % ceria concentration. The morphology and porous structure characteristics confirmed the synthesis of mesoporous titania with anatase crystals. The porous structure, crystalline structure and high absorption in UV light of TiO_2 sample were preserved after cerium impregnation. In presence of cerium the absorption band is shifted to visible light but the intensity decreases between 400 and 600 nm. TGP samples have been successfully used in the photocatalytic degradation of methyl orange in aqueous medium under UV irradiation. The modification of TiO_2 sample surface by cerium oxide decreased its photocatalytic performance in degradation of MO dye under UV light and increased the photocatalytic efficiency in visible light. The best results in photodegradation of MO were obtained for 5% CeO_2 concentration in modified samples.

Acknowledgments: The authors gratefully acknowledge the financial support from the Roumanian National Authority for Scientific Research, CNCS-UEFISCDI; project number PN-III-P2-2.1-PED- 103/2017.

REFERENCES

1. D. Reyes-Coronado, G. Rodriguez-Gattorno, M.E. Espinosa Pesqueira, C. C. R. De Coss and G. Oskam, *Nanotech.*, **2008**, *19*, 1-10.
2. T. Luttrell, S. Halpegamage, J. Tao, A. Kramer, E. Sutter and M. Batzill, *Sci. Rep.,* **2014**, *4*, 4043-4049.
3. G. H. Li, S. Ciston, Z. V. Saponjic, L. Chen, N. M. Dimitrijevic, T. Rajh and K. A. Gray, *J. Catal.*, **2008**, *253*, 105-110.
4. R. Boppella, P. Basak and S. V. Manorama, *ACS Appl. Mater. Interfaces.*, **2012**, *4* , 1239–1246.
5. T. A. Kandiel, A. Feldhoff, L. Robben, R. Dillert and D. W. Bahnemann, *Chem. Mater.,* **2010**, *22*, 2050-2060.
6. R. Boppella, P. Basak and S. V. Manorama, *ACS Appl. Mater. Interfaces*, 2**012**, *4*, 1239-1246.
7. M. T. Laranjo, N. C. Ricardi, L. T. Arenas, E. V. Benvenutti, M. Costa de Oliveira, M. J. L. Santos and T. M. Haas Costa, *J. Sol-Gel Sci. Techn.*, **2014**, *72*, 273–281.
8. P. Kajitvichyanukula, J. Ananpattarachaia and S. Pongpom, *Sci. Technol. Adv. Mat.*, **2005**, *6*, 352–358.
9. S. Segota , L. Curkovic , D. Ljubas, V. Svetlicic , I. F. Houra and N. Tomasic, *Ceram. Int.*, **2011**, *37*, 1153–1160.
10. S. Sahni, S. B. Reddy and B. S. Murty, *Mat. Sci. Eng. A-Struc.*, **2007**, *452-453*, 758-762.
11. Y. V. Kolenko, B. R. Churagulov, M. Kunst, L. Mazerolles and C. Colbeau-Justin, *Appl. Catal. B-Environ.*, **2004**, *54*, 51-58.
12. M. Ouzzine, J. A. Maciá-Agulló, M. A. Lillo-Ródenas, C. Quijada and A. Linares-Solano, *Appl. Catal. B- Environ.,* **2014**, *154-155*, 285-293.
13. P. Yang, D. Zhao, D. I. Margolese, B. F. Chmelka and G. D. Stucky, *Chem. Mater.* **1999,** *11,* 2813-2826.
14. E. M. Samsudin, S. B. Abd Hamid, J. C. Juan and W. J. Basirun, *Appl. Surf. Sci.,* **2015**, *355*, 959–968.
15. N. A. Jadhav, P. K Singh, H.-W. Rhee, S. P. Pandey and B. Bhattacharya*, Int. J. Electrochem. Sci.,***2014**, *9*, 5377 – 5388.
16. C. B. D. Marien, C. Marchal, A. Koch, D. Robert and P. Drogui, *Environ. Sci. Pollut. Res.*, **2017**, *24*, 12582-12588.
17. D. M. Antonelli and J. Y. Ying, *Angew.Chem., Int. Ed. Engl.,* **1995***, 34*, 2014–2017.
18. I.-M. Hung, Y. Wang, C.-F. Huang, Y.-S. Fan, Y.-J. Han and H.-W. Peng, *J. Eur. Ceram. Soc.*, **2010**, *30*, 2065–2072.
19. L. Predoana, I. Stanciu, M. Anastasescu, J. M. Calderon-Moreno, M. Stoica, S. Preda, M. Gartner and M. Zaharescu, *J. Sol-Gel Sci. Techn.*, **2016**, *78*, 589-599.
20. A. Zaleska, *Recent Pat. Eng.*, **2008**, *2*, 157-164.
21. T. Ohno, *Water Sci. Technol*., **2004**, *49*, 159-163.
22. L. Kong, D. J. Gregg, I. Karatchevtseva, Z. Zhang, M. G. Blackford, S. C. Middleburgh, G. R. Lumpkin and G. Triani, *Inorg. Chem.*, **2014**, *53*, 6761–6768.
23. S. A. Ansari, M. M. Khan, M. O. Ansari, S. Kalathil, J. Lee and M. H. Cho, *RSC Adv.***, 2014**, *4*, 16782-16791.
24. M. Zaharescu, A. Wittmar, V. Teodorescu, C. Andronescu, M. Wittmar and M. Veith, *Z. Anorg. Allg. Chem.*, **2009**, *635*, 1915-1938.
25. F. B. Li, X. Z. Li, M. F. Hou, K. W. Cheah and W. C. H. Choy, *Appl. Catal. A- Gen.*, **2005**, *285*, 181–189.
26. D. Tomova, V. Iliev, A. Eliyas and S. Rakovsky, *Sep. Purif. Technol.*, **2015**, *156*, 715-723.
27. B. Liu, X. Zhao, N. Zhang, Q. Zhao, X. He and J. Feng, *Surf. Sci.*, **2005**, *595*, 203-211.
28. C. H. Kao, S. Z. Chen, Y. Luo, W. T. Chiu, S. W. Chiu, I. C. Chen, C. –Y. Lin and H. Chen, *Appl. Surf. Sci.*, **2017,** *396*, 1673-1677.
29. A. Preuss and R. Gruehn, *J. Solid State Chem.*, **1994**, *110*, 363–369.
30. A. Dauscher, P. Wehrer and L. Hilaire, *Catal. Lett.*, **1992**, *14*, 171–183.
31. L. Kong, D. J. Gregg, I. Karatchevtseva, Z. Zhang, M. G. Blackford, S. C. Middleburgh, G. R. Lumpkin and G. Triani, *Inorg. Chem.*, **2014**, *53*, 6761–6768.

32. M. Nolan, S.C. Parker, S.C. Watson and W. Graeme, *Surf. Sci*., **2005**, *595*, 223–232.
33. S. A. Ansari, M. M. Khan, M. O. Ansari, S. Kalathil, J. Lee and M. H. Cho, *RSC Adv.***, 2014**, *4*, 16782-16791.
34. A. Orlov, D.A. Jefferson, N. Macleod and R.M. Lambert, *Catal. Lett.,* **2004**, *92*, 41–47.
35. N.Yan, Z. Zhu, J. Zhang, Z. Zhao and Q. Liu, *Mater. Res. Bull*., **2012**, *47*, 1869-1873.
36. M. Mureseanu, V. Parvulescu, T. Radu, M. Filip and G. Carja, *J. Alloys Compd.*, **2015**, *648*, 864-873.
37. S. Xie, P. Huang, J. J. Kruzic, X. Zeng and H. Qian, *Sci. Rep.,* **2016**, *6*, 21947-21956.